

Three years of Galileo dust data: II. 1993 to 1995

H. Krüger¹, E. Grün¹, D. P. Hamilton², M. Baguhl¹, S. Dermott³, H. Fechtig¹, B. A. Gustafson³, M. S. Hanner⁴, M. Horányi⁵, J. Kissel¹, B. A. Lindblad⁶, D. Linkert¹, G. Linkert¹, I. Mann⁷, J. A. M. McDonnell⁸, G. E. Morfill⁹, C. Polanskey⁴, R. Riemann¹⁰, G. Schwehm¹⁰, R. Srama¹,
and H. A. Zook¹¹

- 1) Max-Planck-Institut für Kernphysik, 69029 Heidelberg, Germany
- 2) University of Maryland, College Park, MD 20742-2421, USA
- 3) University of Florida, Gainesville, FL 32611, USA
- 4) Jet Propulsion Laboratory, Pasadena, California 91109, USA
- 5) Laboratory for Atmospheric and Space Physics, Univ. of Colorado, Boulder, CO 80309, USA
- 6) Lund Observatory, 221 Lund, Sweden
- 7) Max-Planck-Institut für Aeronomie, 37191 Katlenburg-Lindau, Germany
- 8) University of Kent, Canterbury CT2 7NR, UK
- 9) Max-Planck-Institut für Extraterrestrische Physik, 85748 Garching, Germany
- 10) ESTEC, 2200 AG Noordwijk, The Netherlands
- 11) NASA Johnson Space Center, Houston, Texas 77058, USA

Abstract

Between January 1993 and December 1995 the Galileo spacecraft traversed interplanetary space between Earth and Jupiter and arrived at Jupiter on 7 December 1995. The dust instrument onboard the spacecraft was operating during most of the time and data from the instrument were obtained via memory readouts which occurred at rates between twice per day and once per week. All events were classified by an onboard program into 24 categories. Noise events were usually restricted to the lowest categories (class 0). During Galileo's passage through Jupiter's radiation belts on 7 December 1995 several of the higher categories (classes 1 and 2) also show evidence for contamination by noise. The highest categories (class 3) were noise-free all the time. A relatively constant impact rate of interplanetary and interstellar (big) particles of 0.4 impacts per day was detected over the whole three-year time span. In the outer solar system (outside about 2.6 AU) they are mostly of interstellar origin, whereas in the inner solar system they are mostly interplanetary particles. Within about 1.7 AU from Jupiter intense streams of small dust particles were detected with impact rates of up to 20,000 per day whose impact directions are compatible with a Jovian origin. Two different populations of dust particles were detected in the Jovian magnetosphere: small stream particles during Galileo's approach to the planet and big particles concentrated closer

¹Correspondence to: krueger@galileo.mpi-hd.mpg.de

to Jupiter between the Galilean satellites. There is strong evidence that the dust stream particles are orders of magnitude smaller in mass and faster than the instrument's calibration, whereas the calibration is valid for the big particles. Because the data transmission rate was very low, the complete data set for only a small fraction (2525) of all detected particles could be transmitted to Earth; the other particles were only counted. Together with the 358 particles published earlier, information about 2883 particles detected by the dust instrument during Galileo's six years' journey to Jupiter is now available.

1 Introduction

The dust sensors onboard the Galileo and Ulysses spacecraft are highly sensitive impact ionization detectors. The two nearly identical sensors have been described in detail by Grün et al. (1992a,b, 1995a). Results from the dust experiments on both spacecraft have been published frequently: Grün et al. (1992c) published early results from both missions, and dust originating from comets and asteroids has been considered by Riemann and Grün (1992), Hamilton and Burns (1992) and Grün et al. (1994). Dust streams originating from the Jovian system and interstellar dust particles have been discovered with the Ulysses detector (Grün et al. 1993). These were later confirmed by Galileo (Baguhl et al. 1995, Grün et al. 1996a). Grün et al. (1996b) discuss dust particles detected a few days around Galileo's Io flyby on 7 December 1995. During its orbital tour within the Jovian magnetosphere Galileo has demonstrated the electromagnetic interaction of submicron-sized dust particles with Jupiter's magnetic field (Grün et al. 1997, 1998). The data from both instruments – Galileo and Ulysses – have been used to model the interplanetary meteoroid populations (Divine 1993, Grün et al. 1997c) and to compare the mass distribution of interstellar particles derived from in-situ measurements with that obtained from astronomical observations (Baguhl et al. 1996, Landgraf and Grün 1998). Finally, Zook et al. (1996) and Horányi et al. (1997) used data from both spacecraft to model the Jovian dust streams.

This is the fourth paper in a series dedicated to presenting both raw and reduced data from the Galileo and Ulysses dust instruments. Grün et al. (1995a, hereafter Paper I) describe the reduction process of Galileo and Ulysses data. Papers II and III (Grün et al. 1995b,c) contain the data sets from the initial three and two years of the Galileo and Ulysses missions, respectively. In the case of Galileo the time period covered (Paper II) was December 1989 to December 1992. In the current paper we extend the Galileo data set from January 1993 until December 1995. In a companion paper (Krüger et al. 1998, Paper V) we publish the Ulysses data set for the same time period. The main data products are a table of the impact rate of all impacts determined from the particle accumulators and a table of both raw and reduced data of all “big” impacts received on the ground. The information presented in these papers is similar to data which we are submitting to the various

data archiving centers (Planetary Data System, NSSDC, etc.). The only difference is that the paper version does not contain the full data set of the large number of “small” particles. Electronic access to the full data set is also possible via the world wide web: <http://galileo.mpi-hd.mpg.de>.

This paper is organised similarly to Paper II. Section 2 gives a brief overview of the Galileo mission until the end of 1995, the dust instrument and lists important mission events during the 1993 to 1995 period. A description of the Galileo dust data set for 1993 to 1995 together with a discussion of the detected impact rate is given in Sect. 3. Section 4 analyses and discusses various characteristics of the new data set. We dedicate Sect. 5 to an analysis of the dust particles and the noise events detected around Io flyby on 7 December 1995. Finally, Sect. 6 summarizes our results.

2 Mission and instrument operation

Galileo was launched on 18 October 1989. During the initial 3 years of the mission Galileo was in the inner solar system and had flybys of Venus, Earth and the asteroid Gaspra. After its second Earth flyby in December 1992, Galileo had enough energy to leave the inner solar system, fly by the asteroid Ida, and reach Jupiter in December 1995. Galileo’s interplanetary trajectory is shown in Fig. 1 with a few important events indicated: on 28 August 1993 Galileo flew by the asteroid Ida; the atmospheric entry probe was released from the Galileo orbiter on 13 July 1995; on 7 December 1995 Galileo arrived at Jupiter and – after a swing by at Io – was injected into a highly elliptical orbit about the planet. Orbital elements of the Galileo trajectory are provided in Tab. 1. Galileo now performs regular close flybys of Jupiter’s Galilean satellites. A detailed description of the Galileo mission and the spacecraft are given by Johnson et al. (1992) and D’Amario et al. (1992).

Galileo is a dual spinning spacecraft with an antenna that points antiparallel to the positive spin axis. During most of the initial 3 years of the mission the antenna pointed towards the Sun (cf. Fig. 2 in Paper II). Since 1993 the antenna usually points towards Earth. Deviations from the Earth pointing direction between January 1993 and December 1995 are shown in Fig. 2.

The Dust Detector System (DDS) is mounted on the spinning section of Galileo and the sensor axis is offset by an angle of 60° from the positive spin axis (Fig. 3, an angle of 55° has been erroneously used earlier). The rotation angle measures the viewing direction of the dust sensor at the time of a dust particle impact. During one spin revolution of the spacecraft the rotation angle scans through a complete circle of 360° . At rotation angles of 90° and 270° the sensor axis lies nearly in the ecliptic plane, and at 0° it is close to ecliptic north. DDS rotation angles are taken positive around the negative spin axis of the spacecraft. This is done to easily compare Galileo impact spin angle data with those taken by Ulysses, which, unlike

Galileo, has its positive spin axis pointed towards Earth. DDS has a 140° wide field of view and during one spin revolution of the spacecraft the sensor axis scans a cone with 120° opening angle towards the anti-Earth direction. Dust particles that arrive from within 10° of the positive spin axis (anti-Earth direction) can be sensed at all rotation angles, whereas those that arrive at angles from 10° to 130° from the positive spin axis can only be detected over a limited range of rotation angles.

During most of the interplanetary cruise (i. e. prior to 7 December 1995) we received DDS data as instrument memory-readouts (MROs). The MROs returned event data which had accumulated over time in the instrument memory. Initially, an MRO contained 14 instrument data frames (with each frame comprising the complete data set of an impact or noise event, consisting of 128 bits, plus ancillary and engineering data). Since June 1990, when DDS was reprogrammed for the first time after launch, an MRO contains 46 instrument data frames (cf. Paper I). DDS time-tags each impact event with an 8 bit word allowing for the identification of 256 unique times. The step size of this time word was also changed from 1.1 h to 4.3 h in the June 1990 reprogramming to allow for longer time periods between MROs without loss of the impact time information. The total accumulation time is now $256 \times 4.3 \text{ h} = 46 \text{ days}$ after which the time word is reset and the time labels of older impact events become ambiguous. MROs usually occurred twice a week which was sufficient to get the time information of the impact events transmitted to Earth within the 46 day period. The accuracy, however, with which the impact time can be determined, is limited to 4.3 h.

For two periods of a few hours around Io flyby on 7 December 1995 the instrument was read-out every few minutes, the data were stored on Galileo's tape recorder and transmitted to Earth during the following months (record mode). 7 different instrument data frames were read-out this way within about one minute (with 6 frames containing the information of the 6 most recent impact events, the so-called A range, cf. Paper I). Although fewer data frames were read-out in this manner at a time, the number of new events that could be transmitted to Earth in a given time period was much larger than with MROs due to the higher read-out cycle. Furthermore, in record mode the read-out cycle determines the accuracy of the impact time to within a few minutes, much better than with MROs.

Table 2 lists significant mission and dust instrument events for the period 1993 to 1995. A comprehensive list of earlier events can be found in Paper II. After Galileo's second Earth flyby on 8 December 1992, DDS was brought into its nominal operational mode for the rest of the interplanetary cruise to Jupiter: the channeltron voltage was set to 1020 V ($HV = 2$), the event definition status was set such that the channeltron or the ion-collector channel can independently initiate a measurement cycle ($EVD = C, I$) and the detection thresholds for ion-collector, channeltron, electron-channel and entrance grid were set ($SSEN = 0, 0, 1, 1$). Detailed descriptions of these symbols are given in Paper I.

The operational mode of DDS was changed several times during noise tests between

1993 and 1995: starting from the nominal configuration described above, all tests have been achieved with the same instrument settings. The following changes of the instrument configuration were applied at 2 to 3-day intervals: a) increase the channeltron high voltage by one digital step ($HV = 3$); b) reset the channeltron high voltage to its nominal value ($HV = 2$); c) set the event definition status such that the channeltron, the ion collector and the electron-channel can each, independently, initiate a measurement cycle ($EVD = C,I,E$); d) set the thresholds for all channels to their lowest levels ($SSEN = 0, 0, 0, 0$); e) reset the thresholds and the event definition status to their nominal configuration ($SSEN = 0, 0, 1, 1, EVD = C,I$). Note that after step e) DDS is brought back to its nominal configuration. No detectable changes in the noise characteristics were revealed by these noise tests.

The instrument memory was not read out between 3 and 28 July 1995 and no DDS data could be obtained. In this period the atmospheric entry probe was released from the orbiter and a propulsion system burn occurred during the orbit deflection maneuver (ODM) of the orbiter. Within the Jovian magnetosphere a strong increase in the high energy electron flux was expected close to Jupiter. To save the instrument from the hazards associated with Jupiter’s radiation environment the channeltron voltage was reduced and the detection thresholds were increased on 6 December 1995, 5:40h ($HV = 1, EVD = I, SSEN = 2, 0, 2, 2$) at a distance of $30 R_J$ from Jupiter (Jupiter radius, $R_J = 71,492$ km). On 7 December 1995, 23:25h, shortly before insertion of Galileo into Jupiter orbit, the channeltron high voltage was switched off. The Io and Jupiter flybys will be discussed in detail in Sect. 5.

3 Impact events and classification scheme

DDS classifies all events – real impacts of dust particles and noise events – into one of 24 different categories (6 amplitude ranges for the charge measured on the ion collector grid and 4 event classes) and counts them in 24 corresponding accumulators (Paper I). Most of the 24 categories are relatively free from noise and only sensitive to real dust impacts, except for extreme situations like the crossings of the radiation belts of Earth, Venus (Paper II) and Jupiter (7 December 1995, Sect. 5). During most of Galileo’s initial three years of interplanetary cruise since launch only the lowest amplitude and class categories – AC01 (event class 0, amplitude range 1, AR1), AC11, and AC02 – were contaminated by noise events (Paper II).

In a detailed analysis of the Ulysses data set published in Paper III, Baguhl et al. (1993) identified a large number of “small” impacts in the three lowest categories. They deduced a modified event classification scheme that allows for a better discrimination between noise events and real dust impacts. The modified scheme was loaded to the instrument computer on board Galileo during the second reprogramming of DDS on 14 July 1994 and is shown in Tab. 3. The definition of class 3 remains unchanged with respect to the old scheme published in Paper I. Classes 1

and 2 are now divided into two subclasses. With the modified scheme noise events are now usually restricted to class 0. Class 3 always contains good dust impacts (two AC31 events were rejected which occurred during a noise test on 15 August 1995 because they did not fulfill the class 3 classification criteria). After the 14 July 1994 reprogramming, all class 1 and 2 events detected in the low radiation environment of interplanetary space are true dust impacts. Dust impacts which do not fulfill the criteria of classes 1, 2 or 3 are automatically assigned class 0. Therefore, class 0 may still contain good dust impacts, especially in the higher amplitude ranges. Although noise events are now normally restricted to class 0, classes 1 and 2 are also contaminated by noise in extreme radiation environments (Sect. 5). With the modified scheme the mass sensitivity of the instrument could be improved by a factor of eight and the number of dust particles identified in the Ulysses data set from October 1990 to December 1992 was enhanced from 333 to 968 (Baguhl et al. 1993).

Table 4 lists the number of all dust impacts identified with the Galileo dust sensor between 1 January 1993 and 31 December 1995. Before 14 July 1994 the particles were classified with the old classification scheme whereas afterwards the modified scheme was applied. The number of impacts is typically given in intervals of about one week, depending on the occurrence of MROs. When the frequency of MROs was higher or when no impact was recorded, MROs were put together. Typically, MROs occurred twice per week. In interplanetary space where the impact rate was roughly one impact per two days (see below) this was sufficient to receive the complete information of all particles. During the occurrence of dust streams when the impact rates in the lowest amplitude range (AR1) were higher by several orders of magnitude the full information of only a small fraction of all detected particles could be transmitted to Earth. In this case the impact rates had to be deduced from the accumulators.

The frequency of MROs limits the maximum impact rate of dust particles that can be determined from the accumulators. If an unknown number of accumulator overflows occurs between individual MROs the number of particles and, hence, the impact rate deduced is only a lower limit to the real dust impact rate. With MROs occurring every few days, impact rates of up to 100 per day could be determined from the accumulators. Between the end of July and October 1995, when the strongest dust streams were observed, MROs were transmitted to Earth usually daily, sometimes even more frequently. During the occurrence of the most intensive dust streams MROs were split-up and transmitted in two segments separated by about 25 min. This way rates of up to 20,000 impacts per day could be determined from the accumulators over such short time intervals. Entries in Tab. 4 indicated by "#" signs give the number of impacts determined from the accumulators in the lowest amplitude range over the 25 min interval. No overflows of the accumulators for the higher amplitude ranges (AR2 to AR6) occurred between MROs even during the most intensive dust streams. During the strongest dust streams, however,

the effective measurement time for such particles was significantly reduced due to deadtime (cf. Fig 9).

In this paper the terms "small" and "big" do *not* have the same meaning as in Paper II. Here we call all particles in classes 1, 2 and 3 in the amplitude ranges 2 and higher (AR2 to AR6) "big". Particles in the lowest amplitude range (AR1) are called "small". This distinction separates the small Jovian dust stream particles from big particles of interplanetary or interstellar origin (cf. Fig. 9).

The total dust impact rate recorded by DDS from 1993 to 1995 is shown in Fig. 4. During this three year time span the average impact rate of big particles (AR2 to AR6) was rather constant with 0.4 impacts per day. From the beginning of 1993 until the first half of 1994 the average impact rate of small particles (AR1) was about an order of magnitude lower. Later the small particles dominated the overall impact rate. No increase in the impact rate was detected during the Ida flyby on 28 August 1993 and during the passage through the asteroid belt. This is consistent with the absence of an enhanced impact rate during the Gaspra flyby two years earlier, and it is in agreement with the predictions of Hamilton and Burns (1992). DDS detected the first Jovian dust stream on 25 June 1994 with a peak rate of 10 impacts per day. At this time Galileo was still about 1.7 AU away from Jupiter. During the dust streams detected later and closer to Jupiter an impact rate of up to 20,000 per day has been detected. Although such an impact rate is close to the technical limit of Galileo, the data indicate that undetected accumulator overflows did not occur frequently. A detailed discussion of the Jovian dust streams detected with DDS is given by Grün et al. (1996a).

Table 5 lists all 395 big particles detected in classes 1 to 3 between January 1993 and December 1995 for which the complete information exists (Note that this table includes 47 class 1 and 2 events around Io and Jupiter flybys which are possibly noise events, see Sect. 5). We do not list the small particles (AR1) in Tab. 5 because their masses and velocities are outside the calibrated range of DDS. The stream particles are believed to be about 10 nm in size and their velocities exceed 200 km/s (Zook et al. 1996). Any mass and velocity calibration of these particles would be unreliable. The complete information of a total of 2130 small particles has been transmitted to Earth from 1993 to 1995. The full data set of all 2525 small and big particles is available in electronic form.

In Tab. 5 dust particles are identified by their sequence number and their impact time. Gaps in the sequence number are due to the omission of the small particles. The event category – class (CLN) and amplitude range (AR) – are given. Raw data as transmitted to Earth are displayed in the next columns: sector value (SEC) which is the spacecraft spin orientation at the time of impact, impact charge numbers (IA, EA, CA) and rise times (IT, ET), time difference and coincidence of electron and ion signals (EIT, EIC), coincidence of ion and channeltron signal (IIC), charge reading at the entrance grid (PA) and time (PET) between this signal and the impact. Then the instrument configuration is given: event definition (EVD), charge sensing

thresholds (ICP, ECP, CCP, PCP) and channeltron high voltage step (HV). See Paper I for further explanation of the instrument parameters.

The next four columns in Tab. 5 give information about Galileo’s orbit: heliocentric distance (R), ecliptic longitude and latitude (LON, LAT) and distance from Jupiter (D_{Jup}). The next column gives the rotation angle (ROT) as described in Sect. 2. Whenever this value is unknown, ROT is arbitrarily set to 999. This occurs 21 times (80 times in the full data set that includes the small particles). Then follows the pointing direction of DDS at the time of particle impact in ecliptic longitude and latitude (S_{LON} , S_{LAT}). When ROT is not valid S_{LON} and S_{LAT} are also useless. Mean impact velocity (V) and velocity error factor (VEF, i.e. multiply or divide stated velocity by VEF to obtain upper or lower limits) as well as mean particle mass (M) and mass error factor (MEF) are given in the last columns. For $\text{VEF} > 6$, both velocity and mass values should be discarded. This occurs for 5 impacts. No intrinsic dust charge values are given (see Svestka et al. 1996 for a detailed analysis).

4 Analysis

The positive charge measured on the ion collector, Q_{I} , is the most important impact parameter determined by DDS because it is rather insensitive to noise. Figure 5 shows the distribution of Q_{I} for the full data set (small and big particles) from 1993 to 1995. Ion impact charges have been detected over the entire range of six orders of magnitude that the instrument can measure. Two impacts (about 0.1% of the total) are close to the saturation limit of $Q_{\text{I}} \sim 10^{-8}$ C and may thus constitute lower limits of the actual impact charges. The impact charge distribution of the big particles ($Q_{\text{I}} > 10^{-13}$ C) follows a power law with index -0.43 and is shown as a dashed line. This slope is steeper than the value of -1/3 given for Galileo in Paper II and flatter than the -1/2 given for Ulysses in Paper III. It indicates that, on average, Galileo has detected smaller particles in the outer solar system than in the inner solar system. This is in agreement with a larger contribution of interstellar particles further away from the Sun. Note that the Jovian stream particles (AR1) have been excluded from the power law fit.

In Fig. 5 the small particles ($Q_{\text{I}} < 10^{-13}$ C) are put together in two histogram bins. To analyse their behavior in more detail, their number per individual digital step is shown separately in Fig. 6. The distribution flattens for impact charges below 2×10^{-14} C. This indicates that the sensitivity threshold of DDS may not be sharp and the number of impacts with the lowest impact charges Q_{I} may not be complete. The impact charge distribution for these small particles above $Q_{\text{I}} > 2 \times 10^{-14}$ C follows a power law with index -1.9. This indicates that the size distribution of the small stream particles rises steeply towards smaller particles and is much steeper than the distribution of the big particles shown in Fig. 5.

The ratio of the channeltron charge Q_{C} and the ion collector charge Q_{I} is a mea-

sure of the channeltron amplification A which is an important parameter for the dust impact identification (Paper I). The in-flight channeltron amplification was determined in Paper II for the initial three years of the Galileo mission. For a channeltron high voltage of 1020 V ($HV = 2$) the amplification Q_C/Q_I obtained for $10^{-12} \text{ C} \leq Q_I \leq 10^{-10} \text{ C}$ was $A \sim 1.6$. Here we repeat the same analysis for the time period 1993 to 1995 to identify any degrading of the channeltron. Figure 7 shows the charge ratio Q_C/Q_I as a function of Q_I for the same high voltage as in Paper II. The charge ratio Q_C/Q_I determined for $10^{-12} \text{ C} \leq Q_I \leq 10^{-10} \text{ C}$ is $A \sim 1.4$. Thus, no significant aging of the channeltron is detectable. We neglect the large number of small particles in the lowest amplitude range in Fig. 7 because they do not contribute to the determination of the channeltron amplification. Their neglect better illustrates the number distribution of impacts in the higher amplitude ranges.

Figure 8 displays the masses and velocities of all dust particles detected between 1993 and 1995. As in the earlier period (1990 to 1992) velocities occur over the entire calibrated range from 2 to 70 km/s and the masses vary over 10 orders of magnitude from 10^{-6} to 10^{-16} g. The mean errors are a factor of 2 for the velocity and a factor of 10 for the mass. The clustering of the velocity values is due to discrete steps in the rise time measurement but this quantization is much smaller than the velocity uncertainty. Masses and velocities in the lowest amplitude range (particles indicated by plus signs) should be treated with caution. These are mostly Jovian stream particles for which we have clear indications that their masses and velocities are outside the calibrated range of DDS (Zook et al. 1996). The particles are probably much faster and smaller than implied by Fig. 8. On the other hand, the mass and velocity calibration is valid for the bigger particles. For many particles in the lowest two amplitude ranges (AR1 and AR2) the velocity had to be computed from the ion charge signal alone which leads to the striping in the lower mass range in Fig. 8 (most prominent above 10 km/s). In the higher amplitude ranges the velocity could normally be calculated from both the target and the ion charge signal which leads to a more continuous distribution in the mass-velocity plane. Impact velocities below about 3 km/s should be treated with caution because anomalous impacts onto the sensor grids or structures other than the target generally lead to prolonged rise times and hence to artificially low impact velocities.

The sensor orientation (rotation angle) at the time of particle impact is shown in Fig. 9. Particles approaching parallel to the ecliptic plane are detected at rotation angles of 90° and 270° . Contour lines illustrate the detector sensitivity for interstellar particles. The impact direction of most of the big particles (filled circles) is compatible with the interstellar direction. The remaining big particles are compatible with an interplanetary origin. Baguhl et al. (1996) showed that in the outer solar system (i. e. outside about 2.6 AU from the Sun) interstellar particles can be clearly distinguished from particles having interplanetary origin. At distances between 1 and 2.6 AU, however, interplanetary dust particles on prograde orbits approach from the same direction as interstellar particles and both populations can-

not be separated by impact direction arguments. In contrast to the small stream particles which are outside the calibrated range of DDS, the calibration is valid for the interplanetary and interstellar particles (cf. Tab. 5).

The small particles (plus signs) cluster at rotation angles between 200° and 340° which is compatible with a Jovian origin (Grün et al. 1996a). The striping of small impacts (plus signs) is due to the occurrence of individual dust streams and a comparison with Fig. 4 shows that the times of the stripes are coincident with the times of high impact rates. At the end of 1995 the impact rates were so high over several weeks that the symbols form a black area in Fig.9.

5 Io and Jupiter flybys

On 7 December 1995 Galileo arrived at Jupiter after its six years journey through interplanetary space. Because of the expected increase in the high energy electron flux near Jupiter the channeltron high voltage of DDS was reduced and the detection thresholds were increased on 6 December, 5:40 h (Tab. 2). At that time Galileo was at a distance of $15 R_J$ from Jupiter (Jupiter radius, $R_J = 71,492$ km). The change in the instrument configuration led to a reduction in sensitivity by about a factor of six. On 7 December, 17:46 h Galileo flew by Io and at 21:54 h nearest to Jupiter. At 23:25 h the channeltron high voltage was switched off and at 00:27 h on 8 December the orbit insertion maneuver was started which brought Galileo into a bound orbit about Jupiter.

From 1 to 6 December 1995 MROs occurred about once per day. Around the time of Galileo's closest approach to Io on 7 December DDS data were read-out every few minutes and recorded to Galileo's tape recorder (record period, 15:21 h to 18:25 h). After Jupiter closest approach (21:54 h) data were recorded for another two hours (23:22 h to 01:26 h). The recorded data from both flybys were transmitted to Earth a few months later. Initial results from the Io and Jupiter flybys have been published by Grün et al. (1996b).

Figure 10 shows the dust impact rate before and around the Io and Jupiter flybys. During Galileo's approach to Jupiter the impact rate increased considerably and reached a maximum of about 200 impacts per day on 4 December 1995 (day 338). Two days later the sensitivity of the instrument was reduced and the impact rate dropped by about a factor of 10. After the sensitivity reduction a few small particles were still being detected until closest approach to Io. At Io closest approach small particle impacts ceased. Big particles were only detected a few days before closest approach to Io when Galileo was within about $25 R_J$ of Jupiter. The big particles show a concentration towards the inner Jovian system. Impacts of big particles were seen after Io flyby until closest approach to Jupiter, i.e. when impacts of small class 3 particles had already terminated. High impact rates of small particles and increases in the impact rate upon approach towards the inner Jovian system were

also seen later during Galileo’s orbital tour about the planet (Grün et al. 1997, 1998). Concentrations of big particles between the Galilean satellites have also been found. For the calculation of the impact rate in Fig. 10 we have only considered the class 3 impacts because classes 1 and 2 show evidence for contamination by noise in the inner Jovian system (see below). The inclusion of big class 2 events – which seem to be less affected by noise – would increase the number of impacts per given time interval (cf. Tab. 3) but would not change our conclusions about the cessation of small dust impacts after Io and Jupiter flybys (Grün et al. 1996b).

In Fig. 11 we show the rotation angle of the class 3 impacts for which the complete information has been transmitted to Earth. When Galileo was approaching Jupiter the impact directions of dust particles were concentrated between 210° and 350° . About one day before closest approach to Io two particles also arrived from the opposite direction. The striping before day 341 is due to the occurrence of MROs once per day – which allow for a time resolution of 4.3 h – and the fact that the instrument memory of DDS can store only 16 class 3 events. Note that each vertical band of particles between days 332 and 340 in Fig. 11 corresponds to one discrete MRO. If there are more than 16 impacts between two MROs, the oldest events are lost. Before day 341, 15:20 h many class 3 particles have probably been lost. Note that the particle on day 339.0 that caused the peak in the impact rate of big particles in Fig. 10 cannot be shown because its full information has not been transmitted to Earth.

So far we have only considered class 3 impacts around Io and Jupiter flybys. During closest approach to Jupiter in December 1995 and during all later orbits high noise rates occurred when Galileo was within about $20 R_J$ of Jupiter (cf. Grün et al. 1997). In Fig. 12 we show the rotation angle for all impact events in classes 1 to 3 for which the complete information is available for a period of half a day around closest approach to Io. The striping at 15:20 h and 20:40 h is again due to discrete instrument readouts and the time resolution is usually 4.3 h. Because of the switch to record mode which occurred twice on day 341 the impact time can be determined with a higher accuracy from the internal timer of DDS: particles with impact times between 15:10 h and 15:20 h must have impacted the detector between 14:11 h and 15:21 h. Their uncertainty in impact time is only 70 min. Particles with impact times in the time interval 18:30 h to 22:49 h have the full 4.3 h uncertainty, and those with impact times between 23:10 h and 23:22 h must have been detected between 22:49 h and 23:22 h, thus their timing uncertainty is only 33 min.

The class 1 impact events detected about 3 hours before and at Io closest approach itself are spread over the whole range in rotation angles. At the same time the noise counter for the electron channel, which counts all threshold exceedings on that channel, detected a high noise rate in excess of 300 noise events per second. Furthermore, the class 1 event rate is strongly peaked at Io closest approach (Fig. 13). The event rate at Jupiter closest approach cannot be shown because no high resolution recorded data were obtained for that period.

The spread in rotation angle, the increased noise in the electron channel and the peak in impact rate indicate that at least some, if not all, of these events are due to noise rather than dust particle impacts. Although DDS can detect dust particles approaching from within 10° of Galileo's positive spin axis at all rotation angles resulting in a 360° spread in a rotation angle plot, one can hardly imagine a population of dust particles that caused only class 1 events and none in class 3. If the class 1 events are due to real dust particles approaching from close to the positive spin direction, one should also see a similar spread in rotation angle for the class 3 particles which is not the case. The smallest class 2 events (AR1) seem to follow a similar behavior as the class 1 events although much less obvious. Class 2 events also peak at Io closest approach but less strongly which is consistent with class 2 being less contaminated by noise than class 1.

Similar signatures of noise contamination within about $20 R_J$ from Jupiter are evident in the DDS data from Galileo's later orbital tour in the Jovian system (cf. Grün et al. 1997). Therefore, all class 1 and 2 events detected in the Jovian system should be treated with caution. This applies to 26 class 1 and 20 class 2 events in Tab. 5 which were detected on days 341 to 343, and to 50 events in each class if one includes AR1 events and which are published only electronically. Only class 3 events can be considered good dust impacts at the moment. A detailed analysis of the noise characteristics of the DDS data from within the Jovian system is forthcoming.

6 Summary

In this paper, which is the fourth in a series of Galileo and Ulysses papers, we present data from the Galileo dust instrument for the period January 1993 to December 1995 when Galileo was traversing interplanetary space between Earth and Jupiter. The complete information (i. e. all impact parameters measured by the dust instrument) for 395 big particles detected during this period is given (including 47 class 1 and 2 events around Io and Jupiter flybys which are possibly noise events). The full data set that contains 2525 small and big particles is available in electronic form only. Together with the 358 particles published in Paper II a set of 2883 particles detected during Galileo's six years' journey to Jupiter is now available. Our results can be summarized as follows:

- 1) A relatively constant impact rate of interplanetary and interstellar particles of 0.4 impacts per day was detected over the whole three-year time span. In the outer solar system (outside about 2.6 AU) the big particles are mostly of interstellar origin, whereas in the inner solar system interplanetary particles dominate. These particles are in the calibrated mass and velocity range of DDS.
- 2) No increase in impact rate could be detected during the flyby at the asteroid Ida confirming earlier results from the Gaspra flyby.
- 3) Within about 1.7 AU from Jupiter intense streams of small dust particles were

detected with impact rates of up to 20,000 per day whose impact directions are compatible with a Jovian origin. There is strong evidence that the dust stream particles are orders of magnitude smaller in mass and faster than the instrument's calibration, whereas the calibration can be safely applied to the bigger interstellar and interplanetary particles.

4) Two different populations of dust particles were detected in the Jovian magnetosphere: a) small stream particles during Galileo's approach to the planet with impact rates of up to 200 per day 3 days before Io flyby and b) bigger particles concentrated closer to Jupiter between the Galilean satellites.

5) The data from the dust instrument obtained within about $20 R_J$ from Jupiter (Jupiter radius, $R_J = 71,492$ km) show evidence for contamination by noise. The behavior of the impact directions of class 1 and class 2 events differs from that of class 3 events. Class 1 and 2 events from the Jovian system should therefore be treated with caution. Class 3 events do not show any indication for noise contamination and are considered good dust impacts.

6) Noise tests performed regularly during the 3 years period did not reveal any change in the instrument noise characteristics. No degrading of the channeltron was revealed.

Acknowledgments. We thank the Galileo project at JPL for effective and successful mission operations. This work has been supported by the Deutsche Agentur für Raumfahrtangelegenheiten (DARA).

References

Baguhl, M., Grün, E., Linkert, D., Linkert, G. and Siddique, N., Identification of 'small' dust impacts in the Ulysses dust detector data. *Planet. Space Sci.* **41**, No. 11/12, 1085-1098, 1993

Baguhl, M., Grün, E., Hamilton, D.P., Linkert, G., Riemann, R., Staubach, P. and Zook H., The flux of interstellar dust observed by Ulysses and Galileo. *Space Sci. Rev.* **72**, 471-476, 1995

Baguhl, M., Grün, E., Landgraf, M. In situ measurements of interstellar dust with the Ulysses and Galileo spaceprobes. *Space Sci Rev.*, **78**, 165-172, 1996

D'Amario, L.A., Bright, L.E. and Wolf, A.A., Galileo trajectory design. *Space Sci. Rev.* **60**, 23-78, 1992

Divine, N. Five populations of interplanetary meteoroids. *J. Geophys. Res.* **98**, 17029-17048, 1993

Grün, E., Fechtig, H., Hanner, M.S., Kissel, J., Lindblad, B-A., Linkert, D., Linkert, G., Morfill, G.E. and Zook, H.A., The Galileo Dust Detector. *Space Sci. Rev.* **60**, 317-340, 1992a

Grün, E., Fechtig, H., Giese, R.H., Kissel, J., Linkert, D., Maas, D., McDonnell, J.A.M., Morfill, G.E., Schwehm, G. and Zook, H.A., The Ulysses dust experiment. *Astron. Astrophys. Suppl. Ser.* **92**, 411-423, 1992b

Grün, E., Baguhl, M., Fechtig, H., Hanner, M.S., Kissel, J., Lindblad, B.-A., Linkert, D., Linkert, G., Mann, I., McDonnell, J.A.M., Morfill, G.E., Polanskey, C., Riemann, R., Schwehm, G., Siddique, N. and Zook, H.A., Galileo and Ulysses dust measurements: From Venus to Jupiter. *Geophys. Res. Letters* **19**, 1311-1314, 1992c

Grün, E., Zook, H.A., Baguhl, M., Balogh, A., Bame, S.J., Fechtig, H., Forsyth, R., Hanner, M.S., Horanyi, M., Kissel, J., Lindblad, B.-A., Linkert, D., Linkert, G., Mann, I., McDonnell, J.A.M., Morfill, G.E., Phillips, J.L., Polanskey, C., Schwehm, G., Siddique, N., Staubach, P., Svestka, J. and Taylor, A., Discovery of jovian dust streams and interstellar grains by the Ulysses spacecraft. *Nature* **362**, 428-430, 1993

Grün, E., Hamilton, D.P., Baguhl, M., Riemann, R., Horanyi, M. and Polanskey, C., Dust streams from comet Shoemaker-Levy 9? *Geophys. Res. Lett.* **21**, 1035-1038, 1994

Grün, E., Baguhl, M., Fechtig, H., Hamilton, D.P., Kissel, J., Linkert, D., Linkert, G. and Riemann, R., Reduction of Galileo and Ulysses dust data. *Planet. Space Sci.* **43**, 941-951, 1995a (Paper I)

Grün, E., Baguhl, M., Divine, N., Fechtig, H., Hamilton, D. P., Hanner, M. S., Kissel, J., Lindblad, B.-A., Linkert, D., Linkert, G., Mann, I., McDonnell, J. A. M., Morfill, G. E., Polanskey, C., Riemann, R., Schwehm, G., Siddique, N., Staubach P. and Zook, H. A. Three years of Galileo dust data. *Planet. Space Sci.* **43**, 953-969, 1995b (Paper II)

Grün, E., Baguhl, M., Divine, N., Fechtig, H., Hamilton, D.P., Hanner, M.S., Kissel, J., Lindblad, B.-A., Linkert, D., Linkert, G., Mann, I., McDonnell, J.A.M., Morfill, G.E., Polanskey, C., Riemann, R., Schwehm, G., Siddique, N., Staubach, P. and Zook, H.A., Two years of Ulysses dust data. *Planet. Space Sci.* **43**, 971-999, 1995c (Paper III)

Grün, E., Baguhl, M., Hamilton, D. P., Riemann, R., Zook, H. A., Dermott, S., Fechtig, H., Gustafson, B. A., Hanner, M. S., Horanyi, M., Khurana, K. K., Kissel, J., Kivelson, M., Lindblad, B.-A., Linkert, D., Linkert, G., Mann, I., McDonnell, J. A. M., Morfill, G. E., Polanskey, C., Schwehm, G. and Srama, R. Constraints from Galileo observations on the origin of jovian dust streams. *Nature* **381**, 395-398, 1996a

Grün, E., Hamilton, D. P., Riemann, R., Dermott, S., Fechtig, H., Gustafson, B. A., Hanner, M. S., Heck, A., Horányi, M., Kissel, J., Krüger, H., Lindblad, B.-A., Linkert, D., Linkert, G., Mann, I., McDonnell, J. A. M., Morfill, G. E., Polanskey, C., Schwehm, G., Srama, R. and Zook, H. A. Dust measurements during Galileo's approach to Jupiter and Io encounter. *Science* **274**, 399-401, 1996b.

Grün, E., Krüger, H., Dermott, S., Fechtig, H., Graps, A., Gustafson, B. A., Hamilton, D. P., Hanner, M. S., Heck, A., Horányi, M., Kissel, J., Lindblad,

- B.-A., Linkert, D., Linkert, G., Mann, I., McDonnell, J. A. M., Morfill, G. E., Polanskey, C., Schwehm, G., Srama, R. and Zook, H. A. Dust measurements in the jovian magnetosphere. *Geophys. Res. Lett.* **24**, 2171-2174, 1997
- Grün, E., Krüger, H., Graps, A., Hamilton, D. P., Heck, A., Linkert, G., Zook, H. A., Dermott, S., Fechtig, H., Gustafson, B. A., Hanner, M. S., Horányi, M., Kissel, J., Lindblad, B.-A., Linkert, D., Mann, I., McDonnell, J. A. M., Morfill, G. E., Polanskey, C., Schwehm, G., Srama, R. Galileo observes electromagnetically coupled dust in the jovian magnetosphere. *J. Geophys. Res.*, in press, 1998
- Grün, E., Staubach, P., Baguhl, M., Hamilton, D. P., Zook, H. A., Dermott, S., Gustafson, B. A., Fechtig, H., Kissel, J., Linkert, D., Linkert, G., Srama, R., Hanner, M. S., Polanskey, C., Horanyi, M., Lindblad, B.-A., Mann, I., McDonnell, J. A. M., Morfill, G. E. and Schwehm, G. South-north and radial traverses through the zodiacal cloud. *Icarus*, **129**, 270-288, 1997c
- Hamilton, D.P. and Burns, J.A., Orbital stability zones about asteroids II. The destabilizing effects of eccentric orbits and of solar radiation. *Icarus* **96**, 43-64, 1992
- Horányi, M., Grün, E., Heck, A. Modeling the Galileo dust measurements at Jupiter. *Geophys. Res. Lett.* **24**, 2175-2178, 1997
- Johnson, T.V., Yeates, C.M. and Young, R., Space Science Reviews Volume on Galileo Mission Overview. *Space Sci. Rev.* **60**, 3-21, 1992
- Krüger, H., Grün, E., Landgraf, M., Baguhl, M., Dermott, S., Fechtig, H., Gustafson, B. A., Hamilton, D. P., Hanner, M. S., Horányi, M., Kissel, J., Lindblad, B.-A., Linkert, D., Linkert, G., Mann, I., McDonnell, J. A. M., Morfill, G. E., Polanskey, C., Schwehm, G., Srama, R. and Zook, H. A., Three years of Ulysses dust data: 1993 to 1995. *Planet. Space. Sci.*, 1998, this volume (Paper V)
- Landgraf, M. and Grün, E. In situ measurements of interstellar dust. *Proceedings of the IAU Colloquium No. 166 on The Local Bubble and Beyond*, (edited by D. Breitschwerdt, M.J. Freyberg and J. Trümper), Lecture Notes in Physics, Vol. 506, Springer Heidelberg, p. 381-384, 1998
- Riemann, R. and Grün, E. Meteor streams, asteroids and comets near the orbits of Galileo and Ulysses. *Proceeding of the workshop on Hypervelocity Impacts in Space*, (edited by J.A.M. McDonnell), University of Kent at Canterbury, 120-125, 1992
- Svestka, J., Auer, S., Baguhl, M. and Grün, E. Measurements of dust electric charges by the Ulysses and Galileo dust detectors. In: *Physics, Chemistry and Dynamics of Interplanetary Dust*, ASP Conference Series, Vol. 104, (edited by B. A. Gustafson and M. S. Hanner), page 31-34, 1996
- Zook, H. A., Grün, E., Baguhl, M., Hamilton, D. P., Linkert, G., Liou, J.-C., Forsyth, R., Phillips, J. L. Solar wind magnetic field bending of jovian dust trajectories. *Science* **274**, 1501-1503, 1996.

Table 1: Heliocentric orbital elements of Galileo’s interplanetary trajectory for 1993 to 1995. The positional error is less than 500,000 km (= 0.003 AU) from 1 Jan 1993 to 1 Jan 1995. The error increases to 2,500,000 km (= 0.02 AU) by mid 1995 and to 10,000,000 km (= 0.07 AU) by end of 1995. The increasing error is due to the strong influence of Jupiter.

Epoch	4 Sep. 1993, 16:48:00
Perihelion	0.98849 AU
Eccentricity	0.68548
Inclination	1.5169°
Long. of Asc. Node	255.99°
Arg. of Perihelion	186.71°
Mean Anomaly	46.953°
True Anomaly	130.40°

Table 2: Galileo mission and dust detector (DDS) configuration, tests and other events. See text for details. Only selected events are given before 1993.

Yr-day	Date	Time	Event
89-291	18 Oct 1989	16:52	Galileo launch
92-343	08 Dec 1992	15:09	Galileo second Earth flyby
92-343	08 Dec 1992	16:09	DDS configuration: HV=2, EVD=C,I, SSEN=0,0,1,1
92-357	22 Dec 1992	14:59	DDS first MRO after second Earth flyby
93-166	15 Jun 1993		Galileo 80 bytes MRO Format
93-240	28 Aug 1993	16:52	Galileo Ida flyby
93-288	15 Oct 1993	05:42	DDS noise test start
93-301	28 Oct 1993	03:27	DDS noise test end
93-320	16 Nov 1993	03:16	DDS noise test start
93-328	24 Nov 1993	01:58	DDS noise test end
93-355	21 Dec 1993	21:07	DDS noise test start
94-006	06 Jan 1994	20:27	DDS noise test end
94-195	14 Jul 1994	11:00	DDS last MRO before reprogramming
94-195	14 Jul 1994	14:35	DDS counters reset, new event classification program
94-196	15 Jul 1994	02:00	DDS first MRO after reprogramming
94-197	16 Jul 1994		Galileo start SL 9 observations, duration: 6 days
94-210	29 Jul 1994	00:14	DDS noise test start
94-219	07 Aug 1994	08:14	DDS noise test end
94-300	27 Oct 1994	02:38	DDS noise test start
94-312	08 Nov 1994	03:08	DDS noise test end
95-019	19 Jan 1995	22:56	DDS noise test start
95-029	29 Jan 1995	03:09	DDS noise test end
95-035	04 Feb 1995	17:44	Galileo phase 1 software load
95-110	20 Apr 1995	15:19	DDS noise test start
95-119	29 Apr 1995	16:31	DDS noise test end
95-184	03 Jul 1995	04:30	DDS last MRO before probe release
95-194	13 Jul 1995		Galileo probe release
95-205	25 Jul 1995	06:54	DDS configuration for ODM wake-up burn: HV=0
95-205	25 Jul 1995	13:00	DDS configuration: HV=2
95-208	27 Jul 1995	06:54	DDS configuration for ODM wake-up burn: HV=0
95-208	27 Jul 1995	13:00	DDS configuration: HV=2
95-209	28 Jul 1995	06:00	DDS first MRO after probe release
95-221	09 Aug 1995	06:14	DDS noise test start
95-231	19 Aug 1995	05:40	DDS noise test end
95-340	06 Dec 1995	05:00	DDS last MRO before Io and Jupiter flybys
95-340	06 Dec 1995	05:40	DDS configuration: HV=1, EVD=I, SSEN=2,0,2,2
95-341	07 Dec 1995	15:21	Galileo start record data (21 bps DDS data)
95-341	07 Dec 1995	17:46	Galileo Io flyby, altitude: 892 km
95-341	07 Dec 1995	18:25	Galileo end record data

Table 2 continued.

Yr-day	Date	Time	Event
95-341	07 Dec 1995	21:54	Galileo Jupiter closest approach, altitude: 215,000 km
95-341	07 Dec 1995	23:22	Galileo start record data (21 bps DDS data)
95-341	07 Dec 1995	23:25	DDS configuration: HV=off
95-342	08 Dec 1995	00:27	Galileo start orbit insertion burn, duration: 49 min
95-342	08 Dec 1995	01:26	Galileo end record data
95-362	28 Dec 1995	11:00	DDS MRO covering Io and Jupiter flybys

Abbreviations used: MRO: DDS memory read-out; HV: channeltron high voltage step; EVD: event definition, ion- (I), channeltron- (C), or electron-channel (E); SSEN: detection thresholds, ICP, CCP, ECP and PCP; ODM: orbit deflection maneuver; SL 9: comet Shoemaker-Levy 9.

Table 3: Galileo DDS on board classification scheme as derived from the analysis of Baguhl et al. (1993). This scheme was implemented in the instrument computer onboard Galileo during the 14 July 1994 reprogramming. Note that classes 1 and 2 are now divided into two different subclasses which are mutually exclusive. See Paper I for a detailed explanation of the instrument parameters.

Parameters	CLN = 0	CLN = 1		CLN = 2		CLN = 3
Iongrid amplitude (IA)	IA > 0	IA > 0		IA > 0		IA > 0
Target amplitude (EA)	EA > 0	EA > 0		EA > 0		EA > 0
Channeltron amplitude (CA)	CA > 0		CA > 0		CA > 0	CA > 0
Flighttime target-iongrid (EIT)		EIT = 0 or EIT = 15		3 < EIT < 15		3 < EIT < 15
Target-iongrid coincidence (EIC)		EIC = 1		EIC = 0		EIC = 0
Channeltron-iongrid coincidence (ICC)					ICC = 1	ICC = 1
Noise counter of: target (EN) iongrid (IN) channeltron (CN)				EN ≤ 8 IN ≤ 14	CN ≤ 14	EN ≤ 8 IN ≤ 2 CN ≤ 2
EA risetime (ET)						1 ≤ ET ≤ 15
IA risetime (IT)						1 ≤ IT ≤ 15

Date	Time	R [AU]	Δt [d]	AC 01	AC 11	AC 21	AC 31	AC 02	AC 12	AC 22	AC 32	AC 03	AC 13	AC 23	AC 33	AC 04	AC 14	AC 24	AC 34	AC 05	AC 15	AC 25	AC 35	AC 06	AC 16	AC 26	AC 36
94-063	19:09	4.045	8.1	*	*	-	-	*	-	-	2	-	-	-	-	-	-	-	-	-	-	-	-	-	-	-	-
94-074	13:14	4.095	10.8	*	*	-	3	*	2	-	1	-	-	-	1	-	-	-	-	-	-	-	-	-	-	-	-
94-085	13:04	4.145	11.0	*	*	-	4	*	1	-	1	-	-	-	-	-	-	-	-	-	-	-	-	-	-	-	-
94-093	13:05	4.181	8.0	*	*	-	-	*	1	-	-	-	-	-	-	-	-	-	-	-	-	-	-	-	-	-	-
94-101	07:04	4.214	7.7	*	*	-	-	*	-	-	-	-	-	-	3	-	-	-	-	-	-	-	-	-	-	-	-
94-109	07:05	4.249	8.0	*	*	-	3	*	-	-	-	-	-	-	3	-	-	-	-	-	-	-	-	-	-	-	-
94-127	04:51	4.323	17.9	*	*	-	2	*	1	-	2	-	-	-	-	-	-	-	-	-	-	-	-	-	-	-	-
94-135	12:44	4.356	8.3	*	*	-	-	*	-	-	1	-	-	-	2	-	-	-	1	-	-	-	-	-	-	-	-
94-142	14:29	4.384	7.1	*	*	-	1	*	-	-	2	-	-	-	-	-	-	-	-	-	-	-	-	-	-	-	-
94-150	06:14	4.414	7.7	*	*	-	-	*	-	-	1	-	-	-	-	-	-	-	-	-	-	-	-	-	-	-	-
94-161	05:13	4.455	11.0	*	*	-	-	*	1	-	-	-	-	-	2	-	-	-	-	-	-	-	-	-	-	-	-
94-169	06:24	4.485	8.0	*	*	-	2	*	-	-	3	-	-	1	-	1	-	-	-	-	-	-	-	-	-	-	-
94-177	12:38	4.515	8.3	*	*	-	16	*	1	-	1	-	-	-	1	-	-	-	-	-	-	-	-	-	-	-	-
94-185	05:39	4.543	7.7	*	*	-	6	*	1	-	-	-	-	-	-	-	-	-	-	-	-	-	-	-	-	-	-
94-195	10:10	4.578	10.2	*	*	-	-	*	1	-	1	-	-	1	-	-	-	-	-	-	-	-	-	-	-	-	-
94-195	14:05	4.579	0.3	*	3	1	-	*	-	-	-	*	-	-	1	*	-	-	-	*	-	-	-	*	-	-	-
94-203	07:29	4.605	7.9	*	-	-	-	*	-	-	-	*	-	-	-	*	-	-	-	*	-	-	-	*	-	-	-
94-211	22:29	4.633	8.6	*	-	-	-	*	-	2	2	*	-	-	-	*	-	1	-	*	-	-	-	*	-	-	-
94-219	07:21	4.657	7.4	*	-	-	1	*	-	1	-	*	-	-	-	*	-	-	-	*	-	-	-	*	-	-	-
94-266	05:10	4.798	46.9	*	2	22	3	*	2	4	8	*	-	2	6	*	-	-	2	*	-	-	-	*	-	-	-
94-274	19:29	4.822	8.6	*	-	2	-	*	-	2	3	*	-	-	-	*	-	-	-	*	-	-	-	*	-	-	-
94-284	22:05	4.850	10.1	*	-	2	-	*	-	1	3	*	-	1	-	*	-	-	-	*	-	1	-	*	-	-	-
94-292	06:15	4.869	7.3	*	-	3	-	*	-	1	3	*	-	-	-	*	-	-	-	*	-	-	-	*	-	-	-
94-300	01:45	4.889	7.8	*	-	7	-	*	-	1	-	*	-	-	2	*	-	-	-	*	-	-	-	*	-	-	-
94-309	18:30	4.913	9.7	*	-	7	4	*	-	-	3	*	-	-	-	*	-	-	-	*	-	-	-	*	-	-	-
94-318	19:38	4.935	9.0	*	-	2	1	*	1	1	-	*	-	-	1	*	-	-	1	*	-	-	-	*	-	-	-
94-327	02:13	4.954	8.3	*	-	1	1	*	-	-	1	*	-	-	1	*	-	-	-	*	-	-	-	*	-	-	-
94-343	23:53	4.992	16.9	*	1	5	2	*	1	-	3	*	-	-	2	*	-	-	-	*	-	-	-	*	-	-	-
94-351	03:05	5.007	7.1	*	-	1	-	*	-	-	1	*	-	-	-	*	-	-	1	*	-	-	-	*	-	-	-
94-362	02:45	5.030	11.0	*	1	190	39	*	-	-	2	*	-	-	-	*	-	-	1	*	-	-	-	*	-	-	-
95-007	02:21	5.050	10.0	*	2	142	98	*	-	-	1	*	-	-	-	*	-	-	-	*	-	-	-	*	-	-	-
95-021	21:49	5.078	14.8	*	2	5	-	*	-	-	-	*	-	1	-	*	-	-	-	*	-	-	-	*	-	-	-
95-029	02:18	5.091	7.2	*	1	2	-	*	1	2	1	*	-	-	1	*	-	-	-	*	-	-	-	*	-	-	-
95-044	23:23	5.118	15.9	*	1	17	5	*	-	-	-	*	-	-	1	*	-	-	-	*	-	-	-	*	-	-	-
95-061	20:44	5.145	16.9	*	-	39	10	*	-	2	-	*	-	1	1	*	-	-	-	*	-	-	-	*	-	-	-
95-076	23:08	5.168	15.1	*	-	6	-	*	-	2	4	*	-	1	1	*	-	-	-	*	-	-	-	*	-	-	-
95-086	11:29	5.181	9.5	*	1	470	317	*	-	1	1	*	-	-	-	*	-	-	-	*	-	-	-	*	-	-	-
95-096	17:10	5.194	10.2	*	1	598	292	*	-	4	1	*	-	-	-	*	-	-	-	*	-	-	-	*	-	-	-
95-104	18:28	5.204	8.1	*	2	384	278	*	-	1	1	*	-	-	-	*	-	-	-	*	-	-	-	*	-	-	-
95-113	13:58	5.214	8.8	*	1	7	-	*	-	1	-	*	-	-	1	*	-	-	-	*	-	-	-	*	-	-	-

Date	Time	R [AU]	Δt [d]	AC 01	AC 11	AC 21	AC 31	AC 02	AC 12	AC 22	AC 32	AC 03	AC 13	AC 23	AC 33	AC 04	AC 14	AC 24	AC 34	AC 05	AC 15	AC 25	AC 35	AC 06	AC 16	AC 26	AC 36
95-121	12:27	5.223	7.9	*	-	4	2	*	-	-	-	*	-	-	1	*	-	-	-	*	-	-	-	*	-	-	-
95-128	16:24	5.231	7.2	*	-	18	5	*	-	-	-	*	-	-	1	*	-	-	-	*	-	-	-	*	-	-	-
95-138	16:04	5.241	10.0	*	-	8	-	*	-	-	-	*	-	-	-	*	-	-	-	*	-	-	-	*	-	-	-
95-149	16:59	5.251	11.0	*	3	11	-	*	-	1	2	*	-	-	-	*	-	-	-	*	-	-	-	*	-	-	-
95-159	10:28	5.259	9.7	*	-	16	5	*	-	-	-	*	-	-	-	*	-	-	-	*	-	-	-	*	-	-	-
95-166	10:39	5.264	7.0	*	-	8	1	*	-	-	-	*	-	-	-	*	-	-	-	*	-	-	-	*	-	-	-
95-177	12:09	5.272	11.1	*	-	53	10	*	-	-	-	*	-	-	-	*	-	-	-	*	-	-	-	*	-	-	-
95-209	05:59	5.289	31.7	*	-	10 [#]	1 [#]	*	-	2	3	*	-	-	-	*	-	-	-	*	-	-	-	*	-	-	-
95-217	02:31	5.292	7.9	*	-	200 [#]	74 [#]	*	-	1	2	*	-	-	1	*	-	-	-	*	-	-	-	*	-	-	-
95-224	05:17	5.294	7.1	*	-	211 [#]	64 [#]	*	-	5	2	*	-	-	-	*	-	-	-	*	-	-	-	*	-	-	-
95-234	08:39	5.297	10.1	*	-	2 [#]	1 [#]	*	-	4	-	*	-	-	-	*	-	-	1	*	-	-	-	*	-	-	-
95-244	15:44	5.299	10.3	*	-	45 [#]	10 [#]	*	-	5	5	*	-	-	1	*	-	-	-	*	-	-	-	*	-	-	-
95-252	01:36	5.299	7.4	*	-	10 [#]	6 [#]	*	-	1	3	*	-	-	-	*	-	-	-	*	-	-	-	*	-	-	-
95-262	02:07	5.300	10.0	*	-	1 [#]	2 [#]	*	-	1	-	*	-	-	-	*	-	-	-	*	-	-	-	*	-	-	-
95-272	00:56	5.299	10.0	*	-	4 [#]	0 [#]	*	-	1	-	*	-	-	-	*	-	-	-	*	-	-	-	*	-	-	-
95-284	22:28	5.298	12.9	*	-	10 [#]	2 [#]	*	-	1	-	*	-	-	1	*	-	-	-	*	-	-	-	*	-	-	-
95-299	12:48	5.294	14.6	*	1	87	22	*	-	-	3	*	-	-	-	*	-	-	-	*	-	-	-	*	-	-	-
95-323	00:12	5.285	23.5	*	1	100	130	*	1	3	1	*	-	-	-	*	-	-	-	*	-	-	-	*	-	-	-
95-333	00:21	5.280	10.0	*	22	330	293	*	-	1	1	*	-	-	-	*	-	-	1	*	-	-	-	*	-	-	-
95-340	05:37	5.277	7.2	*	264	689	336	*	1	1	1	*	-	-	-	*	-	-	-	*	-	-	-	*	-	-	-
95-341	15:30	5.280	1.4	*	11	40	15	*	52	5	3	*	1	1	1	*	-	-	1	*	-	-	-	*	-	-	-
95-341	17:45	5.281	0.1	*	15	12	1	*	13	7	-	*	1	-	-	*	-	-	-	*	-	-	-	*	-	-	-
95-342	00:11	5.282	0.3	*	86	80	-	*	38	28	-	*	6	3	3	*	4	1	-	*	-	1	1	*	-	1	-
95-362	11:57	5.320	20.5	*	11	9	-	*	53	12	-	*	1	1	-	*	-	-	-	*	1	-	1	*	-	-	-
Impacts (counted)				*	432	3871	2085	*	210	106	116	*	20	14	90	*	12	2	31	*	3	3	8	*	3	1	1
Impacts (complete data)				*	39	847	1244	*	72	68	97	*	12	9	86	*	5	2	30	*	0	2	7	*	3	1	1
All events(complete data)				1533	265	847	1244	127	72	68	97	0	12	9	86	2	5	2	30	0	0	2	7	0	3	1	1

MP. DATE	C LN	AR	S EC	IA	EA	CA	IT	ET	E IT	E IC	I CC	PA	P ET	E VD	I CP	E CP	C CP	P CP	HV	R	LON	LAT	D _{Jup}	ROT	S _{LON}	S _{LAT}	V	VEF	M	MEF
5-341 20:40	2	2	78	8	9	1	7	13	11	0	0	4	28	5	2	2	0	2	1	5.27632	265.0	0.3	0.00201	340	239	49	29.8	1.9	$1.0 \cdot 10^{-14}$	10.5
5-341 20:40	1	2	88	8	0	1	7	0	0	0	0	7	29	5	2	2	0	2	1	5.27632	265.0	0.3	0.00201	326	226	42	29.8	1.9	$1.8 \cdot 10^{-14}$	10.5
5-341 20:40	3	3	95	19	20	13	8	12	10	0	1	38	0	5	2	2	0	2	1	5.27632	265.0	0.3	0.00201	316	220	35	9.7	1.9	$6.8 \cdot 10^{-12}$	10.5
5-341 20:41	2	2	179	8	6	1	7	13	10	0	0	8	28	5	2	2	0	2	1	5.27633	265.0	0.3	0.00201	198	239	-51	29.8	1.9	$6.2 \cdot 10^{-15}$	10.5
5-341 23:27	2	2	37	8	6	1	7	14	10	0	0	6	29	5	2	2	0	2	X	5.27810	265.0	0.3	0.00207	38	304	39	29.8	1.9	$6.2 \cdot 10^{-15}$	10.5
5-341 23:30	2	2	249	8	6	1	7	14	10	0	0	9	28	5	2	2	0	2	X	5.27814	265.0	0.3	0.00208	100	318	-8	29.8	1.9	$6.2 \cdot 10^{-15}$	10.5
5-341 23:32	1	2	196	14	12	0	15	9	0	1	0	42	30	5	2	2	0	2	X	5.27816	265.0	0.3	0.00209	174	272	-55	2.0	1.9	$3.3 \cdot 10^{-10}$	10.5
5-341 23:35	2	6	222	58	60	1	5	5	4	1	1	1	0	5	2	2	0	2	X	5.27819	265.0	0.3	0.00210	138	308	-37	40.9	1.6	$1.9 \cdot 10^{-10}$	6.0
5-342 00:11	2	5	0	49	59	0	7	4	5	0	0	49	0	5	2	2	0	2	X	5.27859	265.0	0.3	0.00224	999	999	999	11.8	11.8	$2.2 \cdot 10^{-09}$	5858.3
5-342 13:56	2	2	0	9	9	1	10	12	11	0	0	17	25	5	2	2	0	2	X	5.28441	265.0	0.3	0.00681	999	999	999	9.7	1.9	$4.5 \cdot 10^{-13}$	10.5
5-342 13:56	1	2	0	9	13	1	14	15	0	1	0	17	30	5	2	2	0	2	X	5.28441	265.0	0.3	0.00681	999	999	999	2.1	1.6	$1.3 \cdot 10^{-10}$	6.0
5-342 18:14	2	2	0	12	7	0	14	15	10	0	0	5	29	5	2	2	0	2	X	5.28559	265.1	0.3	0.00811	999	999	999	2.0	1.9	$1.1 \cdot 10^{-10}$	10.5
5-343 07:11	1	2	60	14	15	1	15	15	0	1	0	41	31	5	2	2	0	2	X	5.28842	265.1	0.3	0.01162	6	271	53	2.0	1.9	$5.1 \cdot 10^{-10}$	10.5
5-343 07:11	2	2	253	10	24	0	7	4	9	0	0	46	0	5	2	2	0	2	X	5.28842	265.1	0.3	0.01162	94	319	-3	29.8	1.9	$1.1 \cdot 10^{-13}$	10.5
5-346 21:28	2	2	219	8	6	0	7	15	11	0	0	0	0	5	2	2	0	2	X	5.29890	265.6	0.3	0.02828	142	306	-40	29.8	1.9	$6.2 \cdot 10^{-15}$	10.5

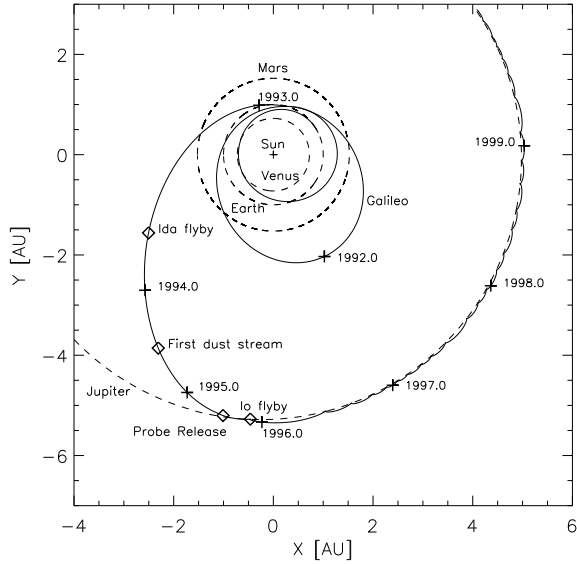


Figure 1: Galileo's interplanetary trajectory from launch until the end of 1999 (solid line) and the orbits of Venus, Earth, Mars and Jupiter (dashed lines). Crosses mark the spacecraft position at the beginning of each year, diamonds indicate special events in the time interval 1993 to 1995 which is the subject of this paper.

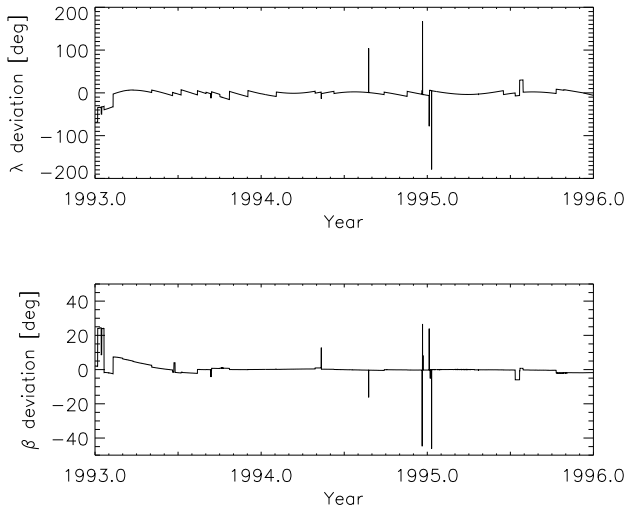


Figure 2: Spacecraft attitude: deviation of the antenna pointing direction (i. e. negative spin axis) from the Earth direction. The angles are given in ecliptic longitude (top) and latitude (bottom, equinox 1950.0).

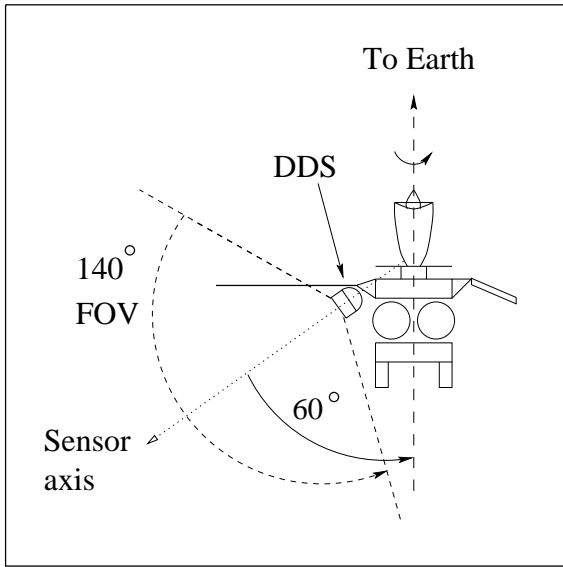


Figure 3: Orientation of Galileo and DDS: the antenna (top) points towards Earth and the dust detector (DDS) largely faces the anti-Earth hemisphere. The sensor axis has an angle of 60° from the positive spin axis (i.e. the anti-Earth direction). During one spin revolution of the spacecraft the sensor axis scans a cone with 120° opening angle. The dust detector itself has 140° field of view (FOV). The sensor orientation shown corresponds to a rotation angle of 270° if viewed from the north ecliptic pole.

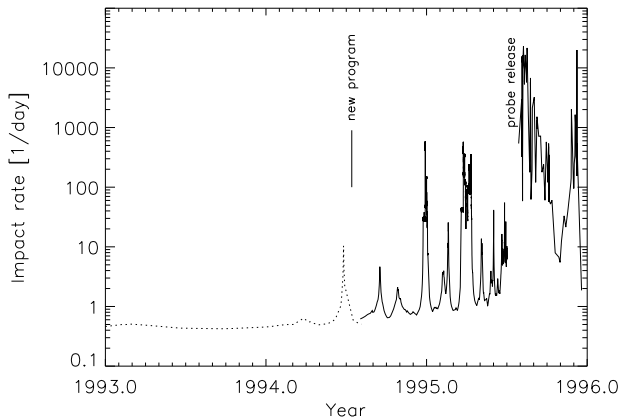


Figure 4: Total dust impact rate detected by DDS as a function of time before (dotted line) and after the reprogramming on 14 July 1994 (solid line). The dotted line is a running average over 9 impacts. The data gap in summer 1995 is due to the release of Galileo's atmospheric entry probe.

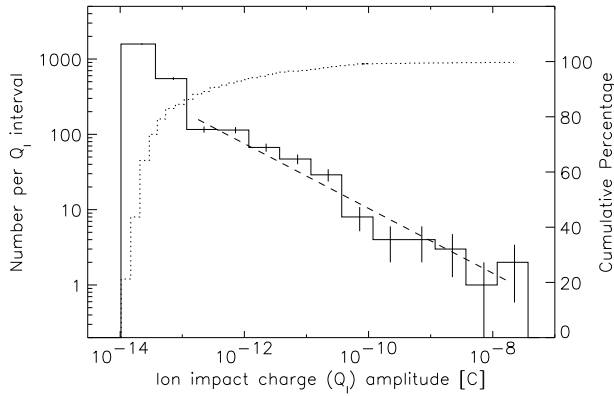


Figure 5: Amplitude distribution of the impact charge Q_I for particles detected between 1993 and 1995. The solid line indicates the number of impacts per charge interval, whereas the dotted line shows the cumulative distribution. Vertical bars indicate the \sqrt{n} statistical fluctuation. A power law fit to the data with $Q_I > 10^{-13}$ C is shown as a dashed line (power law index -0.43).

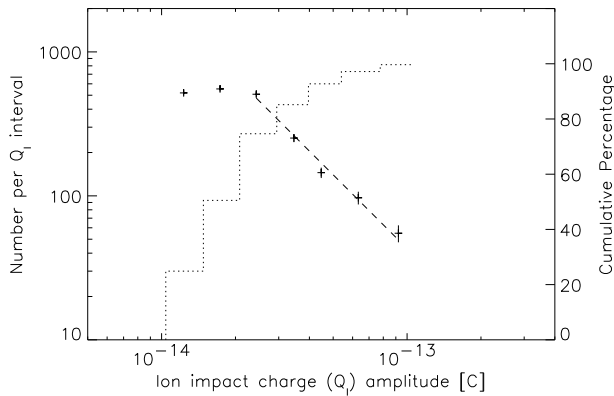


Figure 6: Same as Fig. 5 but for the small particles in the lowest amplitude range (AR1) only. A power law fit to the data with 2×10^{-14} C $< Q_I < 10^{-13}$ C is shown as a dashed line (power law index -1.9).

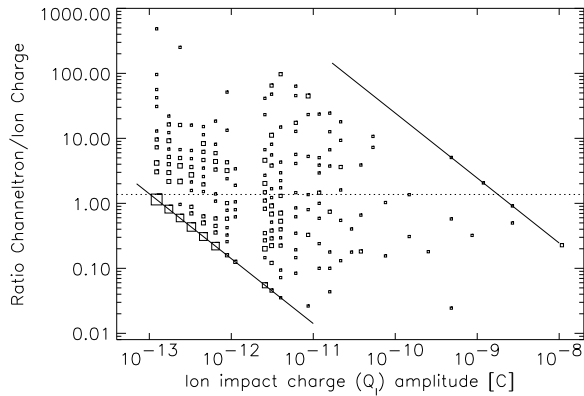


Figure 7: Channeltron amplification factor $A = Q_C/Q_I$ as a function of impact charge Q_I for big particles (AR2 to AR6) detected between 1993 and 1995. The solid lines indicate the sensitivity threshold (lower left) and the saturation limit (upper right) of the channeltron. Squares indicate dust particle impacts and the area of the squares is proportional to the number of events (the scaling of the squares is not the same as in in Paper II). The dotted horizontal line shows the mean value of the channeltron amplification $A = 1.4$ for ion impact charges $10^{-12} \text{ C} < Q_I < 10^{-10} \text{ C}$.

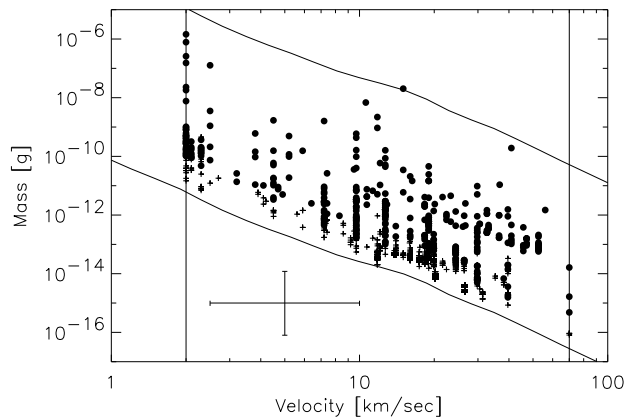


Figure 8: Masses and impact speeds of all impacts recorded by DDS between 1993 and 1995. The lower and upper solid lines indicate the threshold and saturation limits of the detector, respectively, and the vertical lines indicate the calibrated velocity range. A sample error bar is shown that indicates a factor of 2 error for the velocity and a factor of 10 for the mass determination. Note that the small particles (plus signs) are probably faster and smaller than implied by this diagram (see text for details).

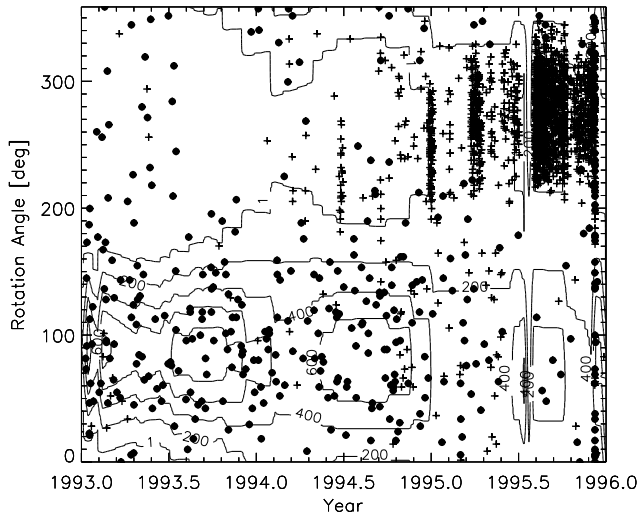


Figure 9: Rotation angle vs. time for two different mass ranges (filled circles: big particles, AR2 to AR6; plus signs: small particles, AR1). See Sect. 2 for an explanation of the rotation angle. The dust streams show up as vertical bands with plus signs. For some time periods no rotation angle information was available; these data are not shown. The contour lines show the sensitive area of DDS for interstellar particles (levels of 1, 200, 400, 600 and 800 cm^2 detector area are shown). The number of big impacts is depressed during the dust streams because of deadtime caused by the large number of small impacts.

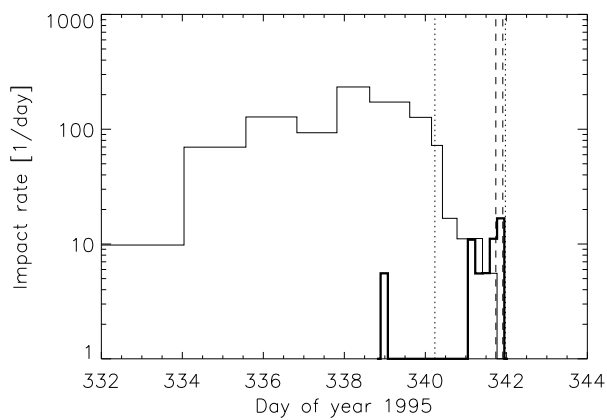


Figure 10: Dust impact rate vs. time for a period of 12 days around Galileo's approach towards the inner Jovian system as obtained from the impact accumulators. The thin solid line shows the impact rate of small particles (AR1) and the heavy solid line shows that of big particles (AR2 to AR6). Because high noise rates in classes 1 and 2 occurred on days 340 to 342 only class 3 impacts are shown here. The times of closest approaches to Io and Jupiter are indicated by dashed lines, and times when the detector sensitivity was reduced are shown as dotted lines. Note that the peak in the impact rate of big particles on day 339.0 is produced by only one impact.

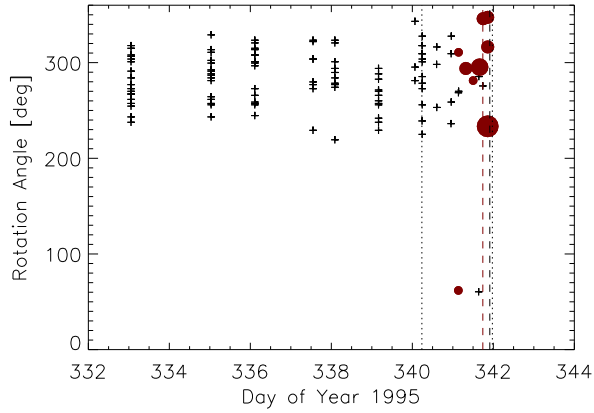


Figure 11: Rotation angle vs. time for 12 days around Galileo's approach towards the inner Jovian system. Only class 3 impacts are shown for which the full information has been transmitted to Earth. Plus signs indicate small particles (AR1) and filled circles show big particles (the symbol size denotes the amplitude range of the particle, AR2 to AR5). The times of closest approaches to Io and Jupiter are indicated by dashed lines, whereas times when the detector sensitivity was reduced are shown as dotted lines. The striping before day 341, 15:20 h is due to the occurrence of MROs once per day which allow for only 4.3 h time resolution and the fact that the instrument memory of DDS can store only 16 class 3 events. Many particles have probably been lost before day 341.

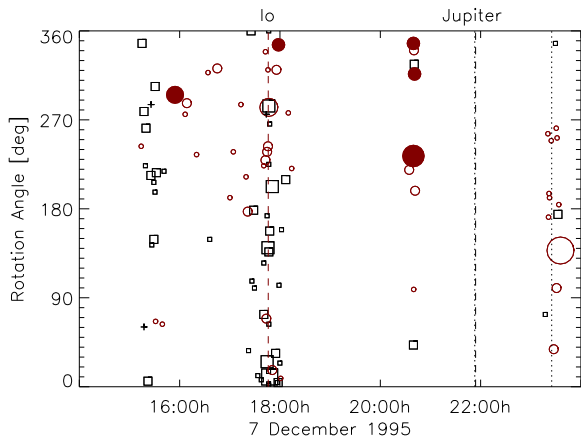


Figure 12: Rotation angle vs. time for a period of 12 h around Io closest approach on 7 Dec 1995 (day 341). The symbols have the following meaning: ”+”: class 3, AR1; ”●“: class 3, AR2 to AR5; ”○” : class 2; ”□“: class 1; The size of the symbols indicates the amplitude ranges of the particles, with AR1 being the smallest and AR6 being the biggest amplitude range occurring in the diagram. The times of closest approaches to Io and Jupiter are indicated by dashed lines and the time when the detector sensitivity was reduced is shown as a dotted line. Events at 20:40 h occurred in a gap when no data have been transmitted to Earth and their impact times have 4.3 h uncertainty. For the other particles the uncertainty in impact time is usually a few minutes, except for impacts at 15:20 h and 23:20 h which have 70 min and 33 min uncertainty, respectively (see text for details).

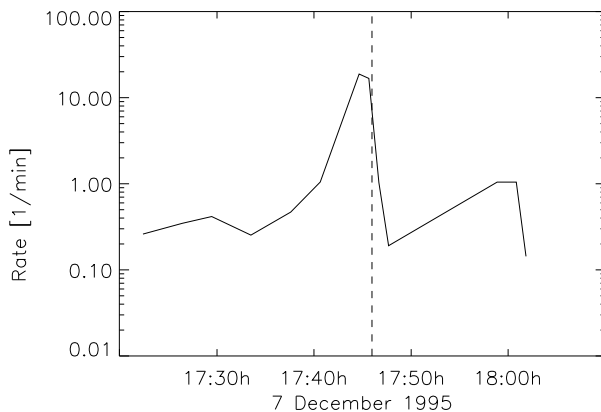


Figure 13: Event rate of class 1 events for a period of 50 min around Io closest approach. The time of closest approach to Io is indicated by a dashed line.

No.	IMP.	DATE	C L N	AR	S E C	IA	EA	CA	IT	ET	E I T	E I C	I C C	PA	P E T	E V D	I C P	E C P	C C P	P C P	HV	R	LON	LAT	D _{Jup}	ROT	S _{LON}	S _{LAT}	V	VEF	M	MEF
844	95-341	20:40	2	2	78	8	9	1	7	13	11	0	0	4	28	5	2	2	0	2	2	5.27632	265.0	0.3	0.00201	340	239	49	29.8	1.9	$1.0 \cdot 10^{-14}$	10.5
845	95-341	20:40	1	2	88	8	0	1	7	0	0	0	0	7	29	5	2	2	0	2	2	5.27632	265.0	0.3	0.00201	326	226	42	29.8	1.9	$1.8 \cdot 10^{-14}$	10.5
846	95-341	20:40	3	3	95	19	20	13	8	12	10	0	1	38	0	5	2	2	0	2	2	5.27632	265.0	0.3	0.00201	316	220	35	9.7	1.9	$6.8 \cdot 10^{-12}$	10.5
847	95-341	20:41	2	2	179	8	6	1	7	13	10	0	0	8	28	5	2	2	0	2	2	5.27633	265.0	0.3	0.00201	198	239	-51	29.8	1.9	$6.2 \cdot 10^{-15}$	10.5
854	95-341	23:27	2	2	37	8	6	1	7	14	10	0	0	6	29	5	2	2	0	2	2	5.27810	265.0	0.3	0.00207	38	304	39	29.8	1.9	$6.2 \cdot 10^{-15}$	10.5
857	95-341	23:30	2	2	249	8	6	1	7	14	10	0	0	9	28	5	2	2	0	2	2	5.27814	265.0	0.3	0.00208	100	318	-8	29.8	1.9	$6.2 \cdot 10^{-15}$	10.5
859	95-341	23:32	1	2	196	14	12	0	15	9	0	1	0	42	30	5	2	2	0	2	2	5.27816	265.0	0.3	0.00209	174	272	-55	2.0	1.9	$3.3 \cdot 10^{-10}$	10.5
861	95-341	23:35	2	6	222	58	60	1	5	5	4	1	1	1	0	5	2	2	0	2	2	5.27819	265.0	0.3	0.00210	138	308	-37	40.9	1.6	$1.9 \cdot 10^{-10}$	6.0
868	95-342	00:11	2	5	0	49	59	0	7	4	5	0	0	49	0	5	2	2	0	2	2	5.27859	265.0	0.3	0.00224	999	999	999	11.8	11.8	$2.2 \cdot 10^{-09}$	5858.3
876	95-342	13:56	2	2	0	9	9	1	10	12	11	0	0	17	25	5	2	2	0	2	2	5.28441	265.0	0.3	0.00681	999	999	999	9.7	1.9	$4.5 \cdot 10^{-13}$	10.5
877	95-342	13:56	1	2	0	9	13	1	14	15	0	1	0	17	30	5	2	2	0	2	2	5.28441	265.0	0.3	0.00681	999	999	999	2.1	1.6	$1.3 \cdot 10^{-10}$	6.0
878	95-342	18:14	2	2	0	12	7	0	14	15	10	0	0	5	29	5	2	2	0	2	2	5.28559	265.1	0.3	0.00811	999	999	999	2.0	1.9	$1.1 \cdot 10^{-10}$	10.5
879	95-343	07:11	1	2	60	14	15	1	15	15	0	1	0	41	31	5	2	2	0	2	2	5.28842	265.1	0.3	0.01162	6	271	53	2.0	1.9	$5.1 \cdot 10^{-10}$	10.5
880	95-343	07:11	2	2	253	10	24	0	7	4	9	0	0	46	0	5	2	2	0	2	2	5.28842	265.1	0.3	0.01162	94	319	-3	29.8	1.9	$1.1 \cdot 10^{-13}$	10.5
882	95-346	21:28	2	2	219	8	6	0	7	15	11	0	0	0	0	5	2	2	0	2	2	5.29890	265.6	0.3	0.02828	142	306	-40	29.8	1.9	$6.2 \cdot 10^{-15}$	10.5

Date	Time	R [AU]	Δt [d]	AC 01	AC 11	AC 21	AC 31	AC 02	AC 12	AC 22	AC 32	AC 03	AC 13	AC 23	AC 33	AC 04	AC 14	AC 24	AC 34	AC 05	AC 15	AC 25	AC 35	AC 06	AC 16	AC 26	AC 36
94-063	19:09	4.045	8.1	*	*	-	-	*	-	-	2	-	-	-	-	-	-	-	-	-	-	-	-	-	-	-	-
94-074	13:14	4.095	10.8	*	*	-	3	*	2	-	1	-	-	-	1	-	-	-	-	-	-	-	-	-	-	-	-
94-085	13:04	4.145	11.0	*	*	-	4	*	1	-	-	-	-	-	-	-	-	-	-	-	-	-	-	-	-	-	-
94-093	13:05	4.181	8.0	*	*	-	-	*	1	-	-	-	-	-	-	-	-	-	-	-	-	-	-	-	-	-	-
94-101	07:04	4.214	7.7	*	*	-	-	*	-	-	-	-	-	-	3	-	-	-	-	-	-	-	-	-	-	-	-
94-109	07:05	4.249	8.0	*	*	-	3	*	-	-	-	-	-	-	3	-	-	-	-	-	-	-	-	-	-	-	-
94-127	04:51	4.323	17.9	*	*	-	2	*	1	-	2	-	-	-	-	-	-	-	-	-	-	-	-	-	-	-	-
94-135	12:44	4.356	8.3	*	*	-	-	*	-	-	-	-	-	-	2	-	-	-	1	-	-	-	-	-	-	-	-
94-142	14:29	4.384	7.1	*	*	-	1	*	-	-	2	-	-	-	-	-	-	-	-	-	-	-	-	-	-	-	-
94-150	06:14	4.414	7.7	*	*	-	-	*	-	-	1	-	-	-	-	-	-	-	-	-	-	-	-	-	-	-	-
94-161	05:13	4.455	11.0	*	*	-	-	*	1	-	-	-	-	-	2	-	-	-	-	-	-	-	-	-	-	-	-
94-169	06:24	4.485	8.0	*	*	-	2	*	-	-	3	-	-	1	-	1	-	-	-	-	-	-	-	-	-	-	-
94-177	12:38	4.515	8.3	*	*	-	16	*	1	-	1	-	-	-	1	-	-	-	-	-	-	-	-	-	-	-	-
94-185	05:39	4.543	7.7	*	*	-	6	*	1	-	-	-	-	-	-	-	-	-	-	-	-	-	-	-	-	-	-
94-195	10:10	4.578	10.2	*	*	-	-	*	1	-	1	-	-	1	-	-	-	-	-	-	-	-	-	-	-	-	-
94-195	14:05	4.579	0.3																								
94-203	07:29	4.605	7.9	*	3	1	-	*	-	-	-	*	-	-	1	*	-	-	-	*	-	-	-	*	-	-	-
94-211	22:29	4.633	8.6	*	-	-	-	*	-	2	2	*	-	-	-	*	-	1	-	*	-	-	-	*	-	-	-
94-219	07:21	4.657	7.4	*	-	-	1	*	-	-	1	*	-	-	-	*	-	-	-	*	-	-	-	*	-	-	-
94-266	05:10	4.798	46.9	*	2	22	3	*	2	4	8	*	-	2	6	*	-	-	2	*	-	-	-	*	-	-	-
94-274	19:29	4.822	8.6	*	-	2	-	*	-	2	3	*	-	-	-	*	-	-	-	*	-	-	-	*	-	-	-
94-284	22:05	4.850	10.1	*	-	2	-	*	-	1	3	*	-	1	-	*	-	-	-	*	-	1	-	*	-	-	-
94-292	06:15	4.869	7.3	*	-	3	-	*	-	1	3	*	-	-	3	*	-	-	-	*	-	-	-	*	-	-	-
94-300	01:45	4.889	7.8	*	-	7	-	*	-	1	-	*	-	-	2	*	-	-	-	*	-	-	-	*	-	-	-
94-309	18:30	4.913	9.7	*	-	7	4	*	-	-	3	*	-	-	-	*	-	-	-	*	-	-	-	*	-	-	-
94-318	19:38	4.935	9.0	*	-	2	1	*	1	1	-	*	-	-	1	*	-	-	1	*	-	-	-	*	-	-	-
94-327	02:13	4.954	8.3	*	-	1	1	*	-	-	1	*	-	-	1	*	-	-	-	*	-	-	-	*	-	-	-
94-343	23:53	4.992	16.9	*	1	5	2	*	1	-	3	*	-	-	2	*	-	-	-	*	-	-	-	*	-	-	-
94-351	03:05	5.007	7.1	*	-	1	-	*	-	-	1	*	-	-	-	*	-	-	1	*	-	-	-	*	-	-	-
94-362	02:45	5.030	11.0	*	1	190	39	*	-	-	2	*	-	-	-	*	-	-	1	*	-	-	-	*	-	-	-
95-007	02:21	5.050	10.0	*	2	142	98	*	-	-	1	*	-	-	-	*	-	-	-	*	-	-	-	*	-	-	-
95-021	21:49	5.078	14.8	*	2	5	-	*	-	-	1	*	-	1	-	*	-	-	-	*	-	-	-	*	-	-	-
95-029	02:18	5.091	7.2	*	1	2	-	*	-	2	1	*	-	-	1	*	-	-	-	*	-	-	-	*	-	-	-
95-044	23:23	5.118	15.9	*	1	17	5	*	-	-	-	*	-	-	1	*	-	-	-	*	-	-	-	*	-	-	-
95-061	20:44	5.145	16.9	*	-	39	10	*	-	2	-	*	-	1	1	*	-	-	-	*	-	-	-	*	-	-	-
95-076	23:08	5.168	15.1	*	-	6	-	*	-	2	4	*	-	1	1	*	-	-	-	*	-	-	-	*	-	-	-
95-086	11:29	5.181	9.5	*	1	470	317	*	-	1	1	*	-	-	-	*	-	-	-	*	-	-	-	*	-	-	-
95-096	17:10	5.194	10.2	*	1	598	292	*	-	4	1	*	-	-	-	*	-	-	-	*	-	-	-	*	-	-	-
95-104	18:28	5.204	8.1	*	2	384	278	*	-	1	1	*	-	-	-	*	-	-	-	*	-	-	-	*	-	-	-
95-113	13:58	5.214	8.8	*	1	7	-	*	-	1	-	*	-	-	1	*	-	-	-	*	-	-	-	*	-	-	-

Date	Time	R [AU]	Δt [d]	AC 01	AC 11	AC 21	AC 31	AC 02	AC 12	AC 22	AC 32	AC 03	AC 13	AC 23	AC 33	AC 04	AC 14	AC 24	AC 34	AC 05	AC 15	AC 25	AC 35	AC 06	AC 16	AC 26	AC 36
95-121	12:27	5.223	7.9	*	-	4	2	*	-	-	-	*	-	-	1	*	-	-	-	*	-	-	-	*	-	-	-
95-128	16:24	5.231	7.2	*	-	18	5	*	-	-	-	*	-	-	1	*	-	-	-	*	-	-	-	*	-	-	-
95-138	16:04	5.241	10.0	*	-	8	-	*	-	-	-	*	-	-	-	*	-	-	-	*	-	-	-	*	-	-	-
95-149	16:59	5.251	11.0	*	3	11	-	*	-	1	2	*	-	-	-	*	-	-	-	*	-	-	-	*	-	-	-
95-159	10:28	5.259	9.7	*	-	16	5	*	-	-	-	*	-	-	-	*	-	-	-	*	-	-	-	*	-	-	-
95-166	10:39	5.264	7.0	*	-	8	1	*	-	-	-	*	-	-	-	*	-	-	-	*	-	-	-	*	-	-	-
95-177	12:09	5.272	11.1	*	-	53	10	*	-	-	-	*	-	-	-	*	-	-	-	*	-	-	-	*	-	-	-
95-209	05:59	5.289	31.7	*	-	10#	1#	*	-	2	3	*	-	-	-	*	-	-	-	*	-	-	-	*	-	-	-
95-217	02:31	5.292	7.9	*	-	200#	74#	*	-	1	2	*	-	-	1	*	-	-	-	*	-	-	-	*	-	-	-
95-224	05:17	5.294	7.1	*	-	211#	64#	*	-	5	2	*	-	-	-	*	-	-	-	*	-	-	-	*	-	-	-
95-234	08:39	5.297	10.1	*	-	2#	1#	*	-	4	-	*	-	-	-	*	-	-	1	*	-	-	-	*	-	-	-
95-244	15:44	5.299	10.3	*	-	45#	10#	*	-	5	5	*	-	-	1	*	-	-	-	*	-	-	-	*	-	-	-
95-252	01:36	5.299	7.4	*	-	10#	6#	*	-	1	3	*	-	-	-	*	-	-	-	*	-	-	-	*	-	-	-
95-262	02:07	5.300	10.0	*	-	1#	2#	*	-	1	-	*	-	-	-	*	-	-	-	*	-	-	-	*	-	-	-
95-272	00:56	5.299	10.0	*	-	4#	0#	*	-	1	-	*	-	-	-	*	-	-	-	*	-	-	-	*	-	-	-
95-284	22:28	5.298	12.9	*	-	10#	2#	*	-	1	-	*	-	-	1	*	-	-	-	*	-	-	-	*	-	-	-
95-299	12:48	5.294	14.6	*	1	87	22	*	-	-	3	*	-	-	-	*	-	-	-	*	-	-	-	*	-	-	-
95-323	00:12	5.285	23.5	*	1	100	130	*	1	3	1	*	-	-	-	*	-	-	-	*	-	-	-	*	-	-	-
95-333	00:21	5.280	10.0	*	22	330	293	*	-	1	1	*	-	-	-	*	-	-	1	*	-	-	-	*	-	-	-
95-340	05:37	5.277	7.2	*	264	689	336	*	1	1	1	*	-	-	-	*	-	-	-	*	-	-	-	*	-	-	-
95-341	15:30	5.280	1.4	*	11	40	15	*	52	5	3	*	1	1	1	*	-	-	1	*	-	-	-	*	-	-	-
95-341	17:45	5.281	0.1	*	15	12	1	*	13	7	-	*	1	-	-	*	-	-	-	*	-	-	-	*	-	-	-
95-342	00:11	5.282	0.3	*	86	80	-	*	38	28	-	*	6	3	3	*	4	1	-	*	-	1	1	*	-	1	-
95-362	11:57	5.320	20.5	*	11	9	-	*	53	12	-	*	1	1	-	*	-	-	-	*	1	-	1	*	-	-	-
Impacts (counted)				*	432	3871	2085	*	210	106	116	*	20	14	90	*	12	2	31	*	3	3	8	*	3	1	1
Impacts (complete data)				*	39	847	1244	*	72	68	97	*	12	9	86	*	5	2	30	*	0	2	7	*	3	1	1
All events(complete data)				1533	265	847	1244	127	72	68	97	0	12	9	86	2	5	2	30	0	0	2	7	0	3	1	1